

AD-A038 426

SOUTHWEST RESEARCH INST SAN ANTONIO TEX

MICROPLASTICITY, TENSILE FAILURE, AND INDENTATION DAMAGE IN UNF--ETC(U)

APR 77 J LANKFORD

SWRI-02-4231-001

F/G 11/2

N00014-75-C-0668

NL

UNCLASSIFIED

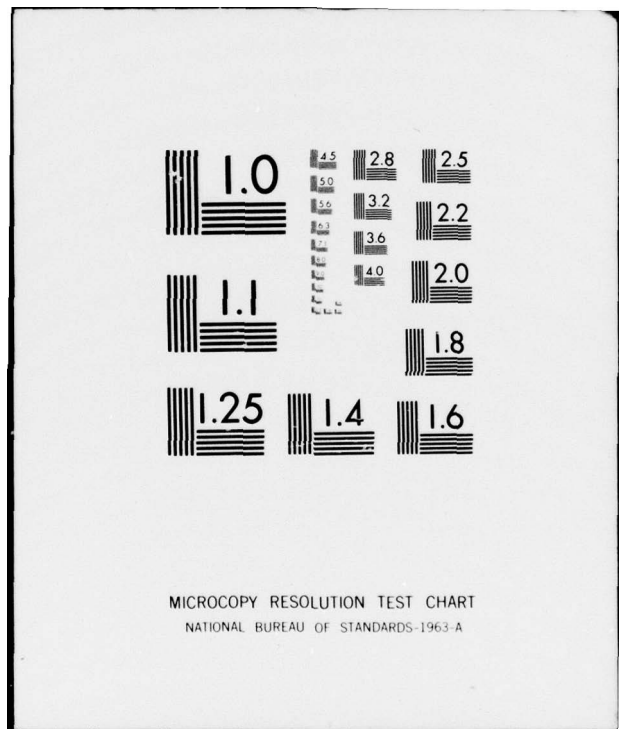
| OF |  
AD  
A038426



END

DATE  
FILMED

5-77



ADA 038426

1

102

# MICROPLASTICITY, TENSILE FAILURE, AND INDENTATION DAMAGE IN UNFLAWED POLYCRYSTALLINE ALUMINA

by

James Lankford, Jr.

## TECHNICAL REPORT

ONR Contract No. N00014-75-C-0668

ONR Contract Authority NR 032-553/1-3-75(471)

SwRI Project No. 02-4231

for

Office of Naval Research  
Arlington, Virginia 22217

by

Southwest Research Institute  
San Antonio, Texas

April 6, 1977

D D C

REF ID: A75747

APR 19 1977

D

Reproduction in whole or in part is permitted for any purpose of the United States Government.

AD NO. 1

DDC FILE COPY



SOUTHWEST RESEARCH INSTITUTE  
SAN ANTONIO      CORPUS CHRISTI      HOUSTON

DISTRIBUTION STATEMENT A

Approved for public release;  
Distribution Unlimited

UNCLASSIFIED

SECURITY CLASSIFICATION OF THIS PAGE (When Data Entered)

REPORT DOCUMENTATION PAGE

READ INSTRUCTIONS  
BEFORE COMPLETING FORM

1. REPORT NUMBER	2. GOVT ACCESSION NO.	3. RECIPIENT'S CATALOG NUMBER								
4. TITLE (and subtitle) MICROPLASTICITY, TENSILE FAILURE, AND INDENTATION DAMAGE IN UNFLAWED POLY- CRYSTALLINE ALUMINA		5. TYPE OF REPORT & PERIOD COVERED Interim Report 1 Apr 76 - 28 Feb 77								
6. AUTHOR(s) James Lankford, Jr		7. PERFORMING ORG. REPORT NUMBER 02-4231-001								
8. CONTRACTOR GRANT NUMBER(s) N00014-75-C-0668										
9. PERFORMING ORGANIZATION NAME AND ADDRESS Southwest Research Institute P. O. Drawer 28510 San Antonio, Texas 78284		10. PROGRAM ELEMENT, PROJECT, TASK AREA & WORK UNIT NUMBERS NR 032-553/1-3-75(471)								
11. CONTROLLING OFFICE NAME AND ADDRESS Office of Naval Research 800 North Quincy Arlington, Virginia 22217		12. REPORT DATE 6 Apr 1977								
13. NUMBER OF PAGES 18 + prelims		14. MONITORING AGENCY NAME & ADDRESS (if different from Controlling Office) 1223p								
15. SECURITY CLASS. (of this report) Unclassified		15a. DECLASSIFICATION/DOWNGRADING SCHEDULE								
16. DISTRIBUTION STATEMENT (of this Report) Distribution is unlimited.										
<div style="border: 1px solid black; padding: 5px; text-align: center;"> <b>DISTRIBUTION STATEMENT A</b>            Approved for public release;            Distribution Unlimited         </div>										
17. DISTRIBUTION STATEMENT (of the abstract entered in Block 20, if different from Report)										
18. SUPPLEMENTARY NOTES										
19. KEY WORDS (Continue on reverse side if necessary and identify by block number) <table style="width: 100%; border-collapse: collapse;"> <tr> <td style="width: 50%;">Microplasticity</td> <td style="width: 50%;">Thermal Activation</td> </tr> <tr> <td>Tensile Strength</td> <td>Acoustic Emission</td> </tr> <tr> <td>Indentation</td> <td>Microcrack Initiation</td> </tr> <tr> <td>Twining</td> <td></td> </tr> </table>			Microplasticity	Thermal Activation	Tensile Strength	Acoustic Emission	Indentation	Microcrack Initiation	Twining	
Microplasticity	Thermal Activation									
Tensile Strength	Acoustic Emission									
Indentation	Microcrack Initiation									
Twining										
20. ABSTRACT (Continue on reverse side if necessary and identify by block number) <p>Scanning electron microscopy and acoustic emission has been used to study microfracture events occurring prior to tensile failure of unflawed <math>Al_2O_3</math> tested at 23° and 410°C. A strengthening effect at the latter temperature is shown to be caused by multiple twinning, and enhanced twinning in general. Twinning is found to be responsible for crack initiation at room temperature. In other experiments, SEM was used to observe microfracture events in <math>Al_2O_3</math> caused by sharp indenters. It was found that lateral crack formation was</p>										

UNCLASSIFIED

SECURITY CLASSIFICATION OF THIS PAGE (When Data Entered)

20. ABSTRACT (Cont'd)

nucleated by mechanical twins located along the inner walls of the indents. The possible relationship of this process to erosion is discussed.



UNCLASSIFIED

SECURITY CLASSIFICATION OF THIS PAGE (When Data Entered)

## FOREWORD

The program on which this report is based is oriented primarily toward assessing the role of compressive stresses and compression-induced damage in the failure of brittle ceramics. During the course of extensive compression testing of polycrystalline alumina, it began to appear likely that the microplastic mechanisms responsible for the observed thermally-activated compressive strength behavior might be responsible for certain aspects of tensile and indentation-related fracture as well. This report summarizes the results of experiments designed to explore these ideas further. A second report will be issued within a few months, in which the results of recent compressive failure and other indentation tests will be presented.

1	2	3	4	5	6	7	8	9	10
11	12	13	14	15	16	17	18	19	20
21	22	23	24	25	26	27	28	29	30
31	32	33	34	35	36	37	38	39	40
41	42	43	44	45	46	47	48	49	50
51	52	53	54	55	56	57	58	59	60
61	62	63	64	65	66	67	68	69	70
71	72	73	74	75	76	77	78	79	80
81	82	83	84	85	86	87	88	89	90
91	92	93	94	95	96	97	98	99	100
101	102	103	104	105	106	107	108	109	110
111	112	113	114	115	116	117	118	119	120
121	122	123	124	125	126	127	128	129	130
131	132	133	134	135	136	137	138	139	140
141	142	143	144	145	146	147	148	149	150
151	152	153	154	155	156	157	158	159	160
161	162	163	164	165	166	167	168	169	170
171	172	173	174	175	176	177	178	179	180
181	182	183	184	185	186	187	188	189	190
191	192	193	194	195	196	197	198	199	200
201	202	203	204	205	206	207	208	209	210
211	212	213	214	215	216	217	218	219	220
221	222	223	224	225	226	227	228	229	230
231	232	233	234	235	236	237	238	239	240
241	242	243	244	245	246	247	248	249	250
251	252	253	254	255	256	257	258	259	260
261	262	263	264	265	266	267	268	269	270
271	272	273	274	275	276	277	278	279	280
281	282	283	284	285	286	287	288	289	290
291	292	293	294	295	296	297	298	299	300
301	302	303	304	305	306	307	308	309	310
311	312	313	314	315	316	317	318	319	320
321	322	323	324	325	326	327	328	329	330
331	332	333	334	335	336	337	338	339	340
341	342	343	344	345	346	347	348	349	350
351	352	353	354	355	356	357	358	359	360
361	362	363	364	365	366	367	368	369	370
371	372	373	374	375	376	377	378	379	380
381	382	383	384	385	386	387	388	389	390
391	392	393	394	395	396	397	398	399	400
401	402	403	404	405	406	407	408	409	410
411	412	413	414	415	416	417	418	419	420
421	422	423	424	425	426	427	428	429	430
431	432	433	434	435	436	437	438	439	440
441	442	443	444	445	446	447	448	449	450
451	452	453	454	455	456	457	458	459	460
461	462	463	464	465	466	467	468	469	470
471	472	473	474	475	476	477	478	479	480
481	482	483	484	485	486	487	488	489	490
491	492	493	494	495	496	497	498	499	500
501	502	503	504	505	506	507	508	509	510
511	512	513	514	515	516	517	518	519	520
521	522	523	524	525	526	527	528	529	530
531	532	533	534	535	536	537	538	539	540
541	542	543	544	545	546	547	548	549	550
551	552	553	554	555	556	557	558	559	560
561	562	563	564	565	566	567	568	569	570
571	572	573	574	575	576	577	578	579	580
581	582	583	584	585	586	587	588	589	590
591	592	593	594	595	596	597	598	599	600
601	602	603	604	605	606	607	608	609	610
611	612	613	614	615	616	617	618	619	620
621	622	623	624	625	626	627	628	629	630
631	632	633	634	635	636	637	638	639	640
641	642	643	644	645	646	647	648	649	650
651	652	653	654	655	656	657	658	659	660
661	662	663	664	665	666	667	668	669	670
671	672	673	674	675	676	677	678	679	680
681	682	683	684	685	686	687	688	689	690
691	692	693	694	695	696	697	698	699	700
701	702	703	704	705	706	707	708	709	710
711	712	713	714	715	716	717	718	719	720
721	722	723	724	725	726	727	728	729	730
731	732	733	734	735	736	737	738	739	740
741	742	743	744	745	746	747	748	749	750
751	752	753	754	755	756	757	758	759	760
761	762	763	764	765	766	767	768	769	770
771	772	773	774	775	776	777	778	779	780
781	782	783	784	785	786	787	788	789	790
791	792	793	794	795	796	797	798	799	800
801	802	803	804	805	806	807	808	809	810
811	812	813	814	815	816	817	818	819	820
821	822	823	824	825	826	827	828	829	830
831	832	833	834	835	836	837	838	839	840
841	842	843	844	845	846	847	848	849	850
851	852	853	854	855	856	857	858	859	860
861	862	863	864	865	866	867	868	869	870
871	872	873	874	875	876	877	878	879	880
881	882	883	884	885	886	887	888	889	890
891	892	893	894	895	896	897	898	899	900
901	902	903	904	905	906	907	908	909	910
911	912	913	914	915	916	917	918	919	920
921	922	923	924	925	926	927	928	929	930
931	932	933	934	935	936	937	938	939	940
941	942	943	944	945	946	947	948	949	950
951	952	953	954	955	956	957	958	959	960
961	962	963	964	965	966	967	968	969	970
971	972	973	974	975	976	977	978	979	980
981	982	983	984	985	986	987	988	989	990
991	992	993	994	995	996	997	998	999	1000

## TABLE OF CONTENTS

	<u>Page</u>
LIST OF ILLUSTRATIONS	v
TENSILE FAILURE OF UNFLAWED POLYCRYSTALLINE $Al_2O_3$	1
1.    Introduction	1
2.    Experimental Procedure	3
3.    Results	3
3.1    Acoustic Emission	3
3.2    Scanning Electron Microscopy	5
4.    Discussion	10
5.    Conclusions	13
References	14
TWINNING AND MICROCRACK NUCLEATION DURING INDENTATION OF ALUMINUM OXIDE	15
1.    Introduction	15
2.    Experiments	15
3.    Results and Discussion	15
References	18

## LIST OF ILLUSTRATIONS

<u>Figure</u>		
<b>"Tensile Failure of Unflawed Polycrystalline <math>Al_2O_3</math>"</b>		
1	Temperature-Atmosphere Effects on the Bend Strength of Lucalox [1]	2
2	Acoustic Emission Count Rate Versus Applied Stress for Lucalox	4
3	Microplasticity (Arrows) Produced Near Tensile Fracture Surface at 23°C	6
4	Comparison of Surface Microplasticity (Arrows) Produced in Tension and Compression at 23°C	7
5	Relationship Between Twinning, Microfracture, and Tensile Failure	8
6	Twinning Under Tensile Loading at 410°C	9
7	Twinning and Twin-Plane Microcracking (Arrow) Under Tension at 410°C	9
8	Multiple Twin Systems Activated in Tension at 410°C	11
9	Possible Twin Facet (Arrow) Near Tensile Fracture Origin (T = 410°C)	11

## "Twinning and Microcrack Nucleation During Indentation of Aluminum Oxide"

1	Indentation Due to 50 gm Load, with Radial Cracks (R) and Twins (Arrows)	17
2	Indentation Due to 100 gm Load, with Radial (R) and Lateral (L) Cracks	17
3	Magnified, Rotated View of Fig. 2, Showing Relationship Between Lateral Crack and Twins	17
4	Conceptual Relationship Between Indentation Twins and Lateral Crack Formation	17

## TENSILE FAILURE OF UNFLAWED POLYCRYSTALLINE $Al_2O_3$

Scanning electron microscopy and acoustic emission are used to investigate the initial stages of tensile failure in unflawed polycrystalline alumina. It is found that deformation twinning plays an important role in crack initiation even at low homologous temperatures, and that the temperature-dependent strength behavior between 23° to 410°C is controlled by twinning.

### 1. Introduction

Polycrystalline aluminum oxide is generally considered to be an archetype brittle ceramic. Yet for many years, it has been known that the tensile strength of  $Al_2O_3$  is characterized by certain behavior occurring at relatively low homologous temperatures whose basis has been laid to at least limited plasticity. Generally, this plasticity has been related to thermally-activated events at the tips of subcritical cracks.

The kind of strength behavior under discussion is shown in Fig. 1 [1], in which it can be seen that the bend strength first decreases with increasing temperature until around 400°C, above which point a dramatic increase in strength is observed. It has been suggested [2-4] that the strength increase might be caused by thermally-enhanced local crack tip plasticity, causing crack blunting or bifurcation. However, detailed TEM study by Weiderhorn, Hockey, and Roberts [5] has demonstrated conclusively the absence of dislocations at the tips of arrested tensile cracks in  $Al_2O_3$ . Manifestation of the strength minimum in vacuo, moreover, indicates that the effect is not environmental. It has been proposed [5] that some sort of thermally-activated complexing at crack tips might provide an explanation, but the possible structure and strength-enhancing mechanism of this "complex" has been discussed only sketchily.

Recently the writer reported the results of experiments in which the compressive strength of a polycrystalline aluminum oxide was determined as a function of strain rate and temperature [6]. The presence of a strength minimum at 200-300°C was reminiscent of the similar effect described above for the tensile case. This suggested that the same mechanism (twin-nucleated microcracking) responsible for the compressive strength minimum might explain the tensile strength behavior as well. Indeed, cursory investigation of a few tensile fractures supported this idea. In this paper, the results of a more detailed look at tensile failure in Lucalox are reported, and are shown to support the suggestion that the strength minimum in unflawed  $Al_2O_3$  is caused by thermally-activated deformation twinning, which in turn controls crack initiation.

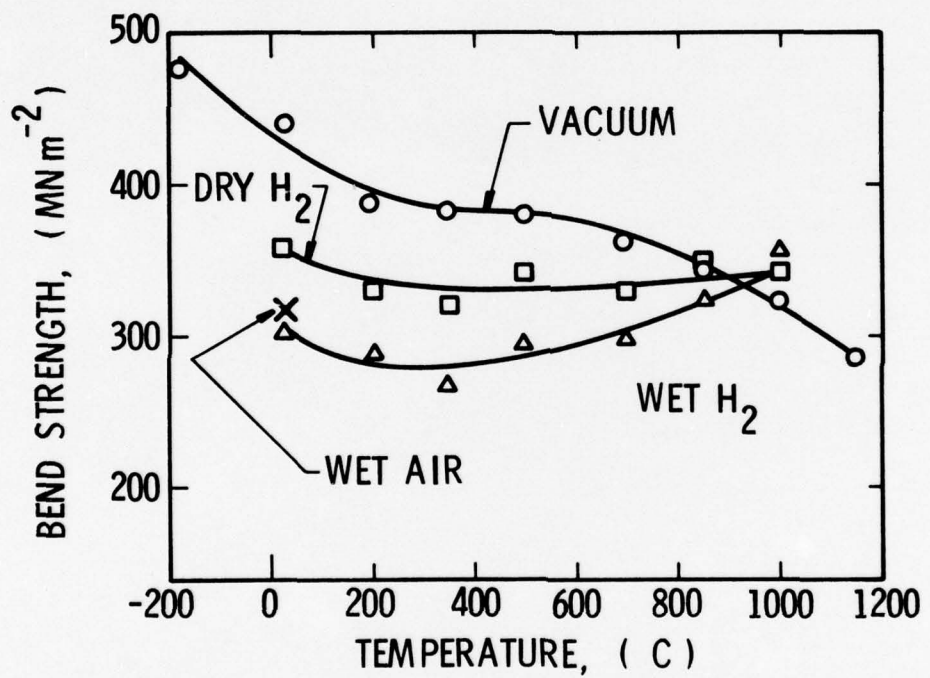


FIGURE 1. TEMPERATURE-ATMOSPHERE EFFECTS ON THE BEND STRENGTH OF LUCALOX [1]

## 2. Experimental Procedure

As-received rods of polycrystalline alumina (type GW Lucalox\*) were cut to length for three-point bending tests, and their ends ground flat for attachment of an acoustic emission transducer. Prior to testing, specimens were cleaned ultrasonically and rinsed in alcohol and distilled water.

Bend tests were carried out at a strain rate of  $1 \times 10^{-5} \text{ sec}^{-1}$ , at temperatures of  $23^\circ$  and  $410^\circ\text{C}$ . Acoustic emission within the frequency domain 100 kHz to 1 MHz was monitored during room temperature testing, using a PZT transducer resonant at 160 kHz (the acoustic emission apparatus and procedures are discussed in detail elsewhere [7]). The acoustic emission detection sensitivity level used in the tensile tests was identical to that used in similar compression tests [7]. The purpose of the three-point bend tests, as opposed to four-point, was to localize any tensile damage and thereby facilitate its detection visually. Similarly, the major goal of the acoustic emission work was to determine the stress level at which tensile damage commenced. In addition, it will be seen that the acoustic emission is helpful in actually assessing the failure micromechanism.

Most of the specimens were tested to failure and then studied in the SEM. A few were loaded to varying sub-failure stress levels and then unloaded for study of early damage. All specimens were coated with palladium for SEM observation.

## 3. Results

### 3.1 Acoustic Emission

A particularly instructive format for utilizing the acoustic emission results is to plot the log of the count rate  $dN/dt$  versus the log of applied stress  $\sigma$ , as shown in Fig. 2. Here, in addition, are shown earlier tensile results by Evans, Linzer, and Russell [8], for as-machined Lucalox, and recent compressive results [7] for the same as-fired Lucalox used in the present study. In all three cases shown, the strain rates and test temperatures are approximately the same. For the tensile-loaded, as-machined material, the slope  $S$  of  $\log dN/dt$  versus  $\log \sigma$  is essentially constant. On the other hand,  $\log dN/dt$ - $\log \sigma$  curve for the as-fired material loaded in tension is divided into two regions of varying slope. The initial value of  $S$  is considerably lower, by a factor of 50%, than for the as-machined Lucalox. At higher stresses, a transition occurs, with  $S$  approximately equal to the as-machined value. It is interesting to observe that during early stages of damage,  $S$  for the as-fired alumina seems to be independent of the mode of loading, i.e., the slope is approximately equal for both compressive and the first stage of tensile loading. However, both the threshold stress ( $\sigma_{AE}$ ) for acoustic emission in tension, and also the initial count rate, are approximately an order of magnitude lower than the corresponding parameters in compression.

\*General Electric Lamp Glass Division, Cleveland, Ohio.

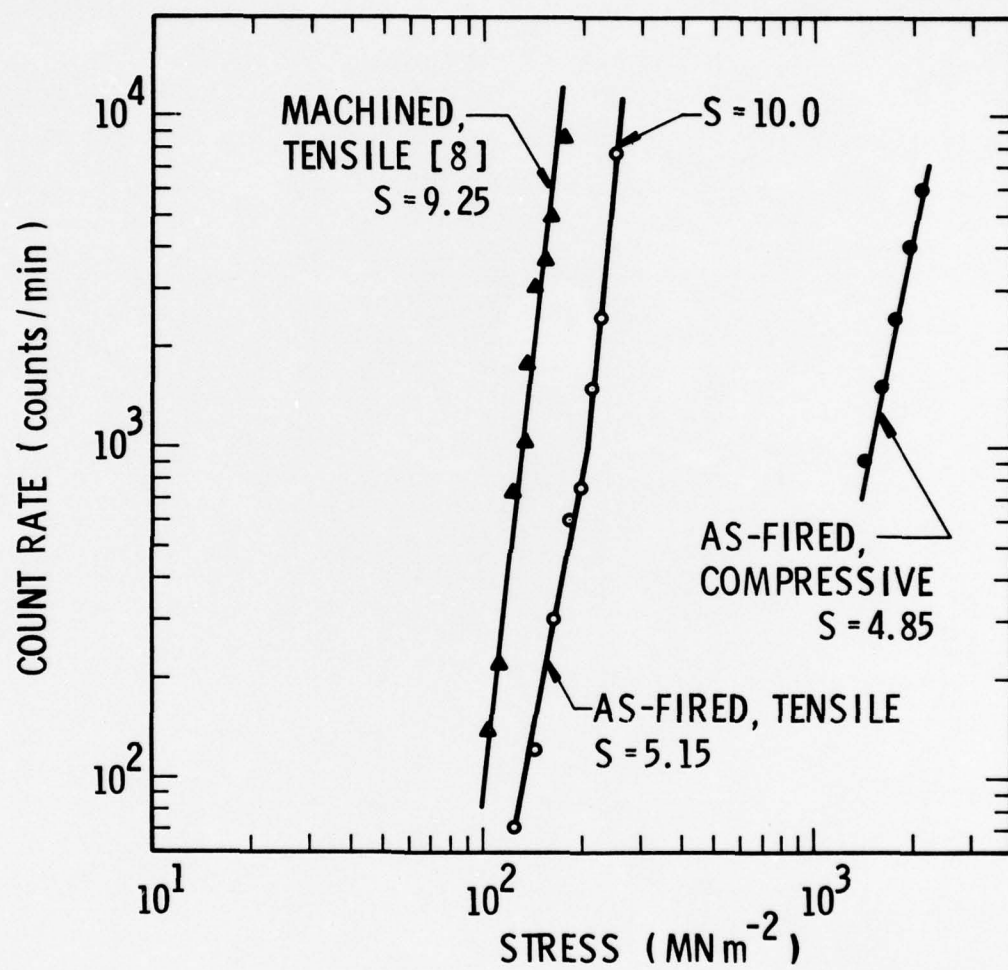


FIGURE 2. ACOUSTIC EMISSION COUNT RATE VERSUS  
APPLIED STRESS FOR LUCALOX

Bend strength ( $\sigma_T$ ) and acoustic emission threshold stress results are summarized in Table 1. The average strength level at 410°C is only slightly lower than that at 23°C, and according to the results of Fig. 1, should reflect the presence of whatever micromechanism is responsible for the general strength increase with rising temperature.

TABLE 1. BEND TEST RESULTS

Temperature (°C)	$\sigma_T$ (MN m <sup>-2</sup> )	$\sigma_{AE}$ (MN m <sup>-2</sup> )
23	215 ± 23	102 ± 17
410	177 ± 25	---

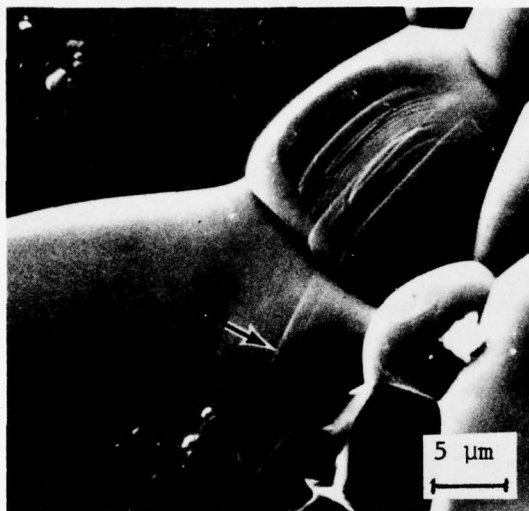
### 3.2 Scanning Electron Microscopy

Prefracture deformation is more difficult to locate at 23°C than at the higher temperature. However, a diligent scanning of regions adjoining the fracture surfaces of specimens failed at room temperature does reveal evidence of microplasticity and indicates its role in the failure process as well.

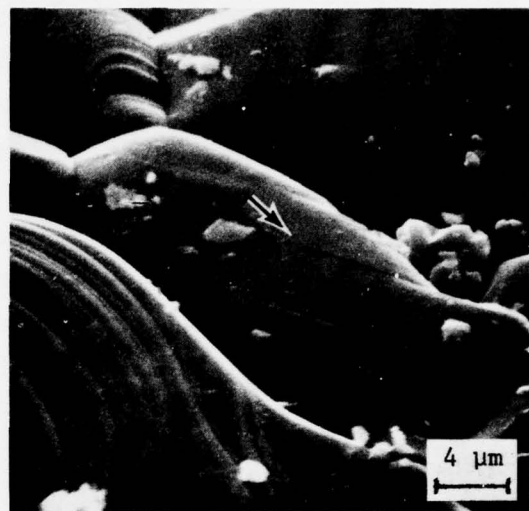
In Fig. 3, several examples of microplasticity produced by uniaxial tensile (bending) stresses at 23°C can be seen. These areas all were located within a few grain diameters of the fracture surface (in each of the photomicrographs to be discussed, the stress axis is vertical). Whether these particular markings reflect twinning or slip cannot be determined with certainty, since they are so narrow. However, they do resemble closely surface deformation produced in the same material by compressive loading, and positively identified as twinning [6]. A comparison between such defects caused by tensile and compressive stresses is shown in Figs. 4a and 4b, respectively. Identification of the compressive flaws as twins was facilitated by the fact that they often are reasonably broad and permit observation of offsets in surface scratches. The tensile twins, particularly at room temperature, seem to be much thinner.

The possible role of the twins in causing tensile failure is suggested by Fig. 5. For the bend specimen shown in Fig. 5a, the apparent fracture origin was the thumbnail region indicated by the arrow. This region was immediately opposite the center support in the three-point bend rig. Near the center of the thumbnail, the grain shown in Fig. 5b was located. This grain exhibits the same twin-like features noted previously, with the fracture plane appearing to wander along several twin planes. Such behavior has been observed during compressive microfracture of Lucalox, and is typical of twin-nucleated cracking [6] in this material.

Similar twinning and twin-related cracking is found for tensile tests carried out at higher temperatures. In Figs. 6 and 7, extensive



(a)



(b)

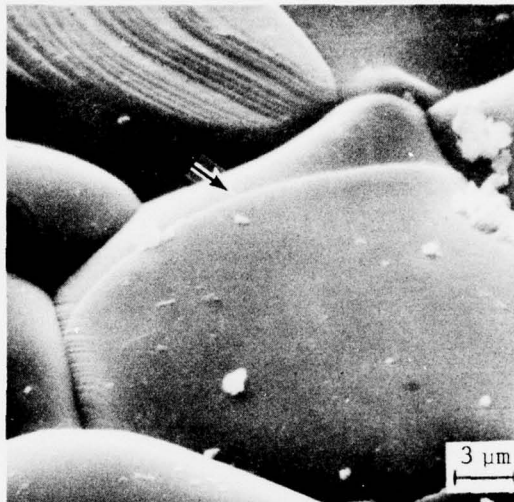


(c)

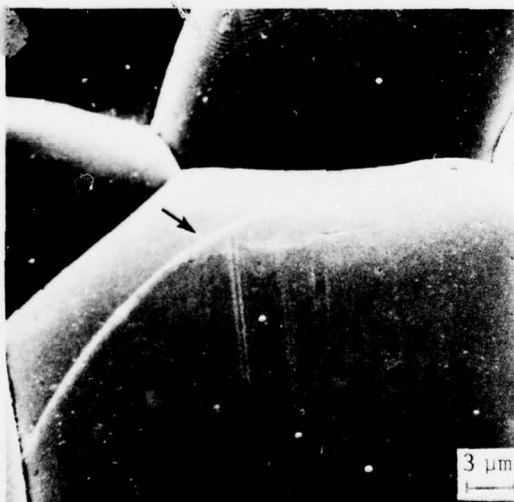


(d)

FIGURE 3. MICROPLASTICITY (ARROWS) PRODUCED NEAR TENSILE FRACTURE SURFACE AT 23°C

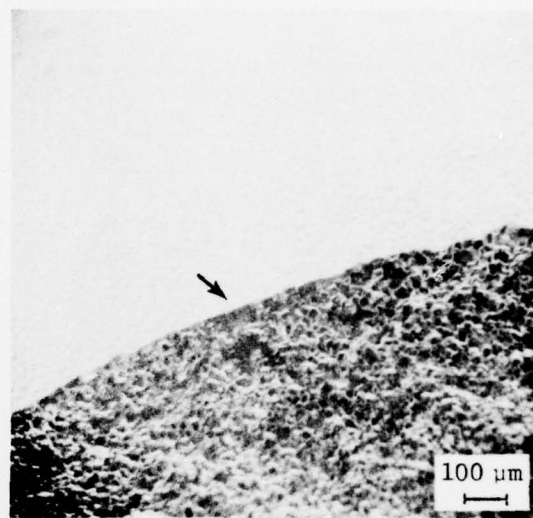


(a) Tensile

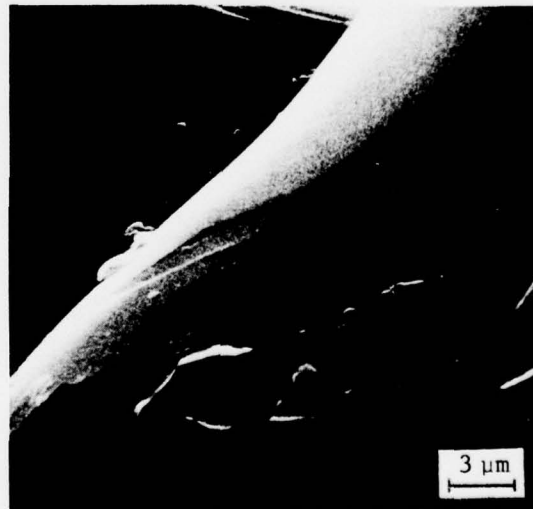


(b) Compressive

FIGURE 4. COMPARISON OF SURFACE MICROPLASTICITY (ARROWS)  
PRODUCED IN TENSION AND COMPRESSION AT 23°C



(a) Fracture surface; arrow indicates origin of failure



(b) Grain associated with initial flaw, showing apparent twin-induced microfracture

FIGURE 5. RELATIONSHIP BETWEEN TWINNING, MICROFRACTURE, AND TENSILE FAILURE

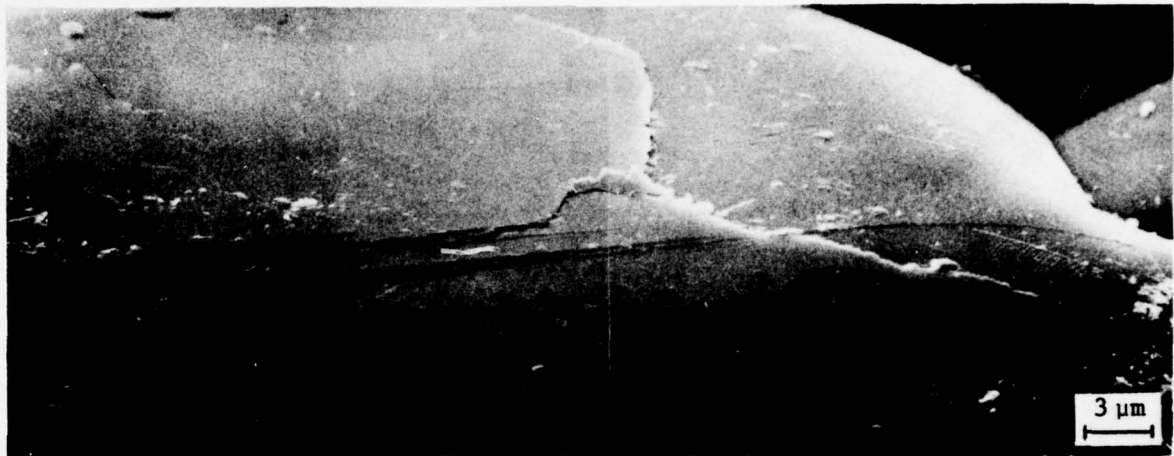


FIGURE 6. TWINNING UNDER TENSILE LOADING AT 410°C

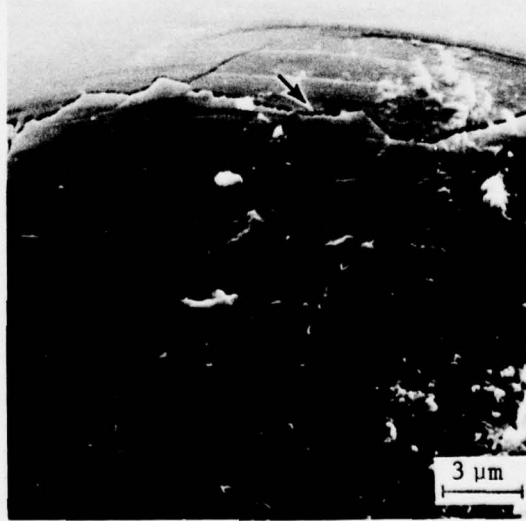


FIGURE 7. TWINNING AND TWIN-PLANE MICROCRACKING (ARROW) UNDER TENSION AT 410°C

fine-scale twinning has occurred in grains adjacent to the major fracture surface, with microcracks having initiated within some of the twins (note the wandering of the crack (C) in Fig. 6b from one twin plane to another). Also at higher temperature, it is observed that multiple twin systems begin to be activated, as was the case during compression testing [7]. This is shown in Fig. 8, where intersecting twins (T) have initiated cracks within (C1) and normal to (C2) twin traces. Some of the twins nucleated at 410°C achieve a significantly greater thickness than those formed at room temperature. These twin facets were often noted near failure nucleation sites; such a location is shown in Fig. 9, in which the local fracture has wandered along a possible twin facet (arrow).

#### 4. Discussion

The first indication that some mechanism other than microcracking alone is responsible for the observed thermally-activated tensile strength behavior can be deduced from the acoustic emission results. Earlier, Evans, et al. [8], had developed an analytical model for acoustic emission due solely to microcracking in bulk specimens. Based on this model, the slope of  $\ln(dN/dt)$  versus  $\ln\sigma$  should be approximately 10. This was found to be the case for their as-machined Lucalox specimens, which contained a large population of prior flaws, i.e., machining cracks, and which gave a slope of 11.7 (Fig. 1). In the present case, the much lower initial slope and the markedly reduced count rate for equivalent stresses point to the operation of some mechanism other than microcracking to account for the early stages of acoustic emission in unflawed  $\text{Al}_2\text{O}_3$ . As noted by Evans, et al. [8], the only other obvious candidates are dislocation motion and twinning. The fact that the compressive and early stages of tensile stressing of unflawed Lucalox produce essentially the same  $\ln(dN/dt)$  versus  $\ln\sigma$  slope implies that the source of acoustic emission is identical in both cases. SEM work previously has proven twinning to be the earliest source during compression [6], and the present electron optical observations are compatible with the same conclusions for tensile failure. However, it is more difficult to separate twinning from possible slip traces in the latter case, since the apparent tensile twins are not as thick as those generated during compression.

Certain work by others is in general agreement with the idea that twinning controls tensile fracture in cases such as the present one. More than ten years ago, Heuer [9] showed that deformation twinning was associated with fracture initiation in corundum single crystals broken in bending at temperatures as low as -196°C. Later, Congleton, et al. [2] showed that there exists a minimum at 250°C in the tensile fracture stress of polycrystalline specimens containing drilled holes. Two possible explanations for this minimum were offered: (1) temperature-dependent crack tip plasticity, or (2) thermally activated crack initiation involving slip or twinning. The TEM work by Weiderhorn, et al. [5], discussed earlier argues against the former. Recently, Becher [10] has shown that the tensile failure of as-ground sapphire bars is controlled by grinding-induced deformation twins, along the habit planes of which the initial microfractures propagate. The implication here is that while grinding introduces several forms of surface damage, including microcracking, slip, and twinning, the propensity for the twin/parent interface to fail under tensile loading, combined with the



FIGURE 8. MULTIPLE TWIN SYSTEMS ACTIVATED IN TENSION AT 410°C. Intersecting twins produce cracks within (C1) and normal to (C2) twin traces.

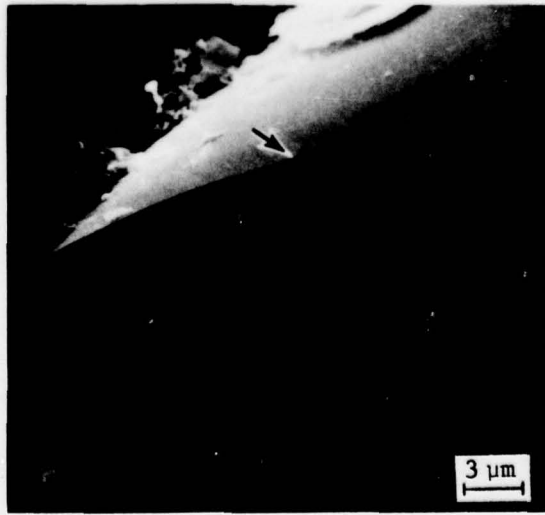


FIGURE 9. POSSIBLE TWIN FACET (ARROW) NEAR TENSILE FRACTURE ORIGIN (T = 410°C)

size of the twins, can cause twinning to dominate as the principal failure mechanism. Finally, deformation markings similar to some of those seen in the present study have been observed by Coble and Parikh [11] on Lucalox deformed in tension. However, the markings at that time could not be unambiguously associated with failure, and their identification as twins was only tentative. The present results indicate the correctness of these earlier speculations [11].

It is interesting to consider the stress levels apparently required for twin nucleation in tension and in compression. Acoustic emission indicates that twinning during tensile loading ( $T = 23^\circ\text{C}$ ,  $\dot{\epsilon} \sim 10^{-5} \text{ sec}^{-1}$ ) commences at around  $130 \text{ MN m}^{-2}$ , while compressive loading under similar conditions requires a stress of  $1400 \text{ MN m}^{-2}$  to initiate twins, as shown in Fig. 2. The reason for this ten-fold strength differential may be related to the inherent stability of flaws nucleated under compression as compared to those formed in tension.

It is possible that during compressive deformation, microtwins actually nucleate at stress levels significantly lower than those detected by the present acoustic emission system. However, it is already well known [6] that flaws such as microcracks, once nucleated in compression, are exceptionally stable and frequently require much higher stress excursions in order to extend. If the stress wave displacement due to initial compressive twinning were below the minimum displacement sensitivity of the acoustic emission system, as might be the case for very small microtwins, then the presence of the twins would be undetected. Detectable acoustic emission would then occur at higher stresses when the twins are driven completely across grains, which is generally accomplished without cracking the twin/parent boundary; rather, it is more common in compression [6] for cracks to nucleate at twin/grain boundary intersections. Usually the twins are stable enough to grow sidewise to achieve a finite thickness. On the other hand, microtwins formed in tension may be less stable. They usually are very thin, tend to extend completely across grains, and often are microcracked along the twin/parent boundary. A suggested scenario is one in which the first twins nucleated in tension zip across a grain as soon as they are formed, accompanied by stress wave emission. Upon reaching a critical size on the order of the grain size, the weak twin/parent interface frequently parts in tension, which effectively precludes further thickening of the twin. At higher stress levels, these cracked twins themselves begin to serve as active flaws, causing crack initiation and extension in adjacent grains. Thus, they can from this level on be considered as "microcracks," whose acoustic emission response undergoes a change from that characteristic of twinning to that corresponding to microcrack extension. This is manifested in the  $S$  value for higher stresses being approximately equal to that found by Evans, et al. [8], for initially microcracked (machined) specimens.

The fact that twinning begins to occur on multiple systems at higher temperatures explains the observed temperature dependent strengthening effect. Plastic accommodation at local stress concentrations through multiple twinning reduces the necessity for crack formation. Moreover, cracks which do occur in such multiple twin fields tend to interfere and interact with one another rather than running neatly across each twinned grain. This

could reduce the propensity for further crack extension in such regions, thereby effectively raising the failure stress.

##### 5. Conclusions

The temperature-dependent strength behavior of unflawed polycrystalline alumina in the temperature range 23°C to 410°C is caused by deformation twinning through its role in microcrack initiation. The twinning is responsible for acoustic emission, whose count rate is dependent upon stress according to the same relationship observed for twinning in compression. The strengthening effect at higher temperatures is caused by enhanced twinning generally, and multiple twin system activity in particular, which aids in accommodating local strain concentration.

## REFERENCES

1. R. J. Charles, Studies of the Brittle Behavior of Ceramic Materials, ASD-TR-61-628 (1963) 467.
2. J. Congleton, N. J. Petch, and S. A. Shiels, Phil. Mag. 19 (1969) 795.
3. J. Congleton and N. J. Petch, Acta Met. 14 (1966) 1179.
4. R. W. Guard and P. C. Romo, Jour. Am. Cer. Soc. 48 (1965) 7.
5. S. M. Wiedenhorn, B. J. Hockey, and D. E. Roberts, Phil. Mag. 28 (1973) 783.
6. J. Lankford, Jour. Mat. Sci. (in press).
7. J. Lankford, Proceedings of the Second International Symposium on the Fracture Mechanics of Ceramics (to be published).
8. A. G. Evans, M. Linzer, and L. R. Russell, Jour. Mat. Sci. 15 (1974) 253.
9. A. H. Heuer, Phil. Mag. 13 (1966) 379.
10. P. F. Becher, Jour. Am. Cer. Soc. 59 (1976) 59.
11. R. L. Coble and N. M. Parikh, Fracture, Vol. VII, ed. H. Liebowitz, Academic Press, N. Y. (1972) 243.

## TWINNING AND MICROCRACK NUCLEATION DURING INDENTATION OF ALUMINUM OXIDE

### 1. Introduction

Indentation fracture recently has been characterized in terms of the sequence of formation and the morphologies of cracks produced during point indentation of brittle solids [1,2]. TEM observations by Hockey [3] and Hockey and Lawn [4] have demonstrated the presence of micro-plastic damage zones beneath indentations in several brittle materials, and Hurley [5] has observed slip-like surface features adjacent to indentations. Hockey [3] has obtained surface terraces, on etching indent sites, whose directions correspond to possible slip and twin traces. However, the relationship between plastic deformation and crack initiation remains unclear, and presently only the extension of certain types of indentation cracks can be predicted, using the fracture mechanics approach [6].

During penetration by a sharp indenter, two kinds of cracks are nucleated; the first to form, known as radial or median vent cracks, extend into the solid along indent diagonals. Initiation occurs on the loading half-cycle, within the inelastic subsurface zone. On the unloading half-cycle, other cracks are nucleated near the surface, in the vicinity of the elastic-plastic boundary. Growth of these lateral cracks is away from the indent and roughly parallel to the surface before curving up to intersect it. Of these two types of fracture, lateral cracking is thought to be relevant to material removal during solid particle erosion.

It has been suggested by Evans and Wilshaw [6] that lateral cracking in particular may be initiated by flaws generated during plastic deformation of the region subsurface to the indenter (this suggestion is supported by the independence of the lateral crack formation load with respect to surface condition). It is the purpose of this report to demonstrate the validity of this idea for alumina.

### 2. Experiments

As-fired Lucalox rods were indented statically with a diamond pyramid indenter. Individual grains, of average dimension 40  $\mu\text{m}$ , were selected for multiple indentation at sequentially higher loads, with the indent orientation maintained constant within a given grain. Following indentation, the specimens were coated with palladium for study in the scanning electron microscope.

### 3. Results and Discussion

For loads of 10 gm and less, indentations are formed with no observable (at 20.000X) cracking. However, faint evidence of plasticity is visible along the inner walls of the indentation, in the form of a regular pattern of banding. These bands are more readily visible at higher loads, as shown

in Fig. 1, where other features also are of interest. Radial cracking begins at loads in excess of 10 gm, with the radial cracks being associated with the indentation corners; they do not appear to extend to the bottom of the indent until loads of several hundred gm are attained.

Plastic "deformation bands" are found along the indentation walls, as well as on the specimen surface adjacent to the indent, as shown in Fig. 1 (arrows). Recent work [7] indicates that twinning is the earliest stage of damage in this same material when stressed in uniaxial compression or tension at 23°C. It also is known that indentation produces a compressive stress state on the indent facets, and tension in the surrounding surface region [6]. Hence, it is likely that the observed indentation plasticity consists of deformation twins. In support of this suggestion, Hockey [8] has observed through TEM that whereas the bulk of the plastic damage in sapphire is confined below the indentation, microtwins often extend upward from this region to the surface.

It has been shown [7] that the twin planes in Lucalox are preferred fracture planes, along which cracks may initiate in both tension and compression. Under indentation loading, they appear to serve as lateral crack nuclei for loads of 100 gm and greater. In Fig. 2, a lateral crack has formed at the left edge of the indent crater, with the center section of the crack, along the edge of the indent, being exceptionally straight. Rotation of the viewing angle by 90° (Fig. 3) shows that this section corresponds to the intersection of an apparent deformation twin with the rim of the indent, below which other non-cracked twins (probably lenticular in shape [3]) are visible. The crack extends laterally over a distance of about 5  $\mu\text{m}$ , as determined by viewing the specimen optically and focusing below the surface to image the crack plane. The conceptual relationship between twinning and crack formation is sketched in Fig. 4.

This type of deformation-induced cracking was observed consistently, its repeatability being further evidence of the role played by the indentation plastic zone, as opposed to pre-existing flaws. For a given crystallite and indenter orientation, the crack initiation pattern at multiple indents was almost identical, i.e., the initial lateral cracking always occurred on a specific, preferred side of each indent, and each crack usually could be identified with a twin trace. At higher loads, lateral cracks begin to nucleate at other sides, also in a repeatable sequence.

The fact that the twins required for lateral crack initiation are present early on implies that the critical load for macrocrack formation does not correspond to that needed to nucleate a twin. Rather, it is more likely that the occurrence of a critical microcrack extension load is based on the statistical probability of crack extension along the twin plane, which increases with the volume of stressed material [6]. The critical extension load is a function of grain orientation relative to the indenter, since this factor controls the angular relationship between the unloading tensile stress field and the most favorable twin plane, on which the twins have formed during the loading indent cycle. This is reflected in variation in the lateral crack extension load by approximately 50% for varying indenter/crystallite orientations.

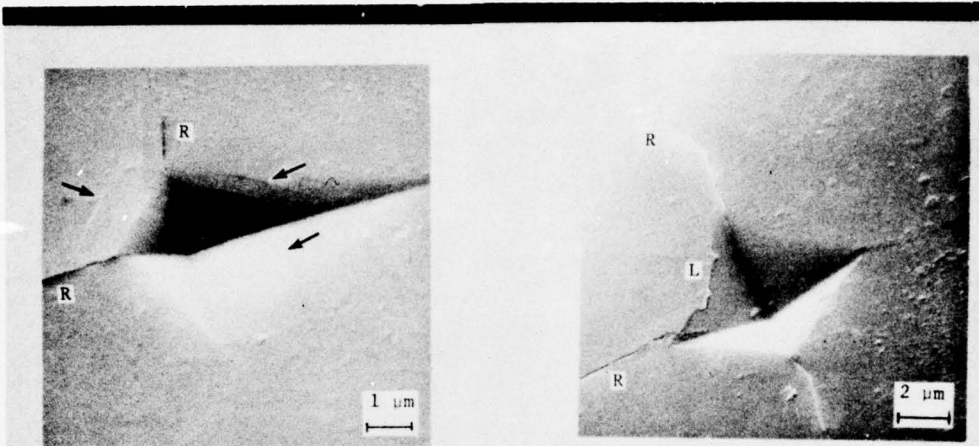


FIG. 1

Indentation due to 50 gm load, with radial cracks (R) and twins (arrows).

FIG. 2

Indentation due to 100 gm load, with radial (R) and lateral (L) cracks.

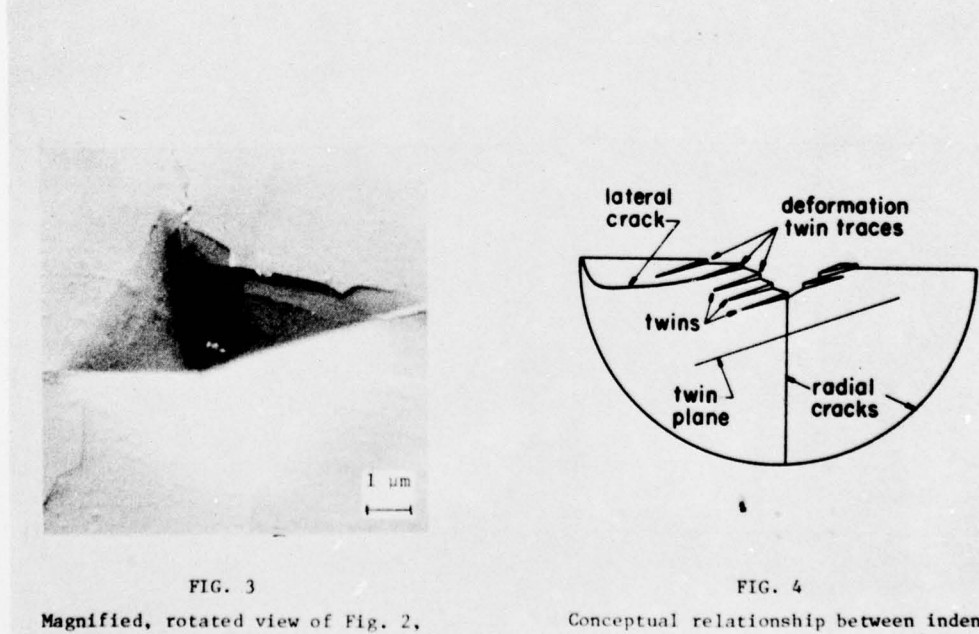


FIG. 3

Magnified, rotated view of Fig. 2, showing relationship between lateral crack and twins (curved slightly due to inelastic indent relaxation).

FIG. 4

Conceptual relationship between indentation twins and lateral crack formation.

## REFERENCES

1. B. Lawn and R. Wilshaw, Jour. Mat. Sci. 10, 1049 (1975).
2. B. R. Lawn and M. V. Swain, Jour. Mat. Sci. 10, 113 (1975).
3. B. J. Hockey, Jour. Amer. Cer. Soc. 54, 223 (1971).
4. B. J. Hockey, Jour. Mat. Sci. 10, 1275 (1975).
5. G. F. Hurley, Met. Trans. 1, 2029 (1970).
6. A. G. Evans and T. R. Wilshaw, Acta Met. 24, 939 (1976).
7. J. Lankford, Jour. Mat. Sci. (in press).
8. B. J. Hockey, private communication (1976).